JOURNAL OF AIRCRAFT
Vol. 39, No. 1, January–February 2002

Equivalent Level of Safety Approach to Damage-Tolerant Aircraft Structural Design

K. Y. Lin,* David T. Rusk,† and Jiaji Du‡
University of Washington, Seattle, Washington 98195-2400

A theoretical approach to damage-tolerant structural design has been proposed based on a probabilistic characterization of relative structural safety. The equations necessary to quantify damage-tolerant structural safety are developed, and their use in the design of a generic composite sandwich panel are demonstrated. Structural safety is identified by the term level of safety, which is defined, for a single inspection event, as the compliment of the probability that a single flaw size larger than the critical flaw size for residual strength of the structure exists and that the flaw will not be detected. The equations derived from this definition incorporate a probabilistic treatment of damage sizes and inspection capabilities. Utilizing damage size data from existing composite aircraft components along with the level of safety, formulas, design charts for residual strength vs safety of a generic composite sandwich panel were constructed. An example design problem is presented that demonstrates the sensitivity of the facesheet thickness sizing parameters to the relative safety of the design. Bayesian statistical techniques are also incorporated to enable the subsequent use of service inspection data to reduce uncertainty in the damage size distributions and to update the structural level of safety value as service experience is acquired.

Nomenclature

A	=	random variable for damage size
a	=	sample damage size from domain A
a_c	=	critical damage size
a_{50}	=	median detection probability for log-odds probability of detection model
D	=	binary random variable for damage detection state, value of 1 means damage is detected
E_1	=	modulus in fiber direction
E_2	=	modulus in matrix direction
$f_A(a)$	=	probability density function of A
G_{12}	=	shear modulus
i	=	damage location
j	=	damage type
k	=	shape factor for log-odds probability of detection model
N_L	=	total number of damage locations
N_{Ti}	=	total number of damage types at ith location
n	=	number of sample damage sizes used for Bayesian updating, or number of flaws present in binomial distribution
$P(Y)$	=	probability of Y
$P_D(a)$	=	probability of detection for damage size a
$p(a)$	=	probability density function of actual damage size
$p_0(a)$	=	probability density function of detected damage size
s^2	=	sample variance of new damage size data
X	=	strength in fiber direction
y	=	log of detected damage size
$\bar{y}$	=	sample mean of new damage size data
Z	=	random variable for number of damages present in structure
z	=	sample damage number from domain Z
γ_{LT}	=	maximum shear strain
ε_L	=	maximum longitudinal strain
ε_T	=	maximum transverse strain
θ	=	scale parameter for lognormal detected damage size distribution
μ	=	number of flaws present in structure, or log of the detected damage scale parameter
ν_{12}	=	Poisson's ratio
σ	=	shape parameter for lognormal detected damage size distribution

Received 2 March 2000; accepted for publication 1 February 2001.

*Professor, Department of Aeronautics and Astronautics, Box 352400.
†Graduate Research Assistant, Department of Aeronautics and Astronautics.
‡Visiting Scientist, Department of Aeronautics and Astronautics.

Introduction

TRADITIONAL design procedures for aircraft structures are based on a combination of factors of safety for loads and notch, scatter, or knockdown factors for strength. Both the factors of safety and knockdown factors have been obtained from the past five decades of design experience on metal aircraft. There are at least two fundamental shortcomings to this approach. First, because they were developed for conventional configurations, metallic materials, and familiar structural concepts, these traditional procedures may be difficult to apply to aircraft that have unconventional configurations, use new material systems, or contain novel structural concepts. A second shortcoming is that measures of safety and reliability are not available for existing airframe components. As a result, it is not possible to determine with any precision the relative importance of various design options on the safety of the aircraft. This situation can lead to excessive weight with no corresponding improvement in overall safety.

Probability and statistical techniques can be applied to the design of damage tolerant structures and would allow a direct comparison to be made between two competing designs based on quantitative values for structural safety. A significant body of research has been conducted on the application of probabilistic design methodologies to composite aircraft structures. Gray and Riskalla[1] and Long and Narciso[2] have recently compiled two excellent summaries of resulting capabilities. Most of this work is focused on developing general design tools for integrated probabilistic modeling of loads, geometry, material properties, and failure mechanisms. Rouchon's work[3] and the work at the Russian Central Aerohydrodynamic Institute[4] are some of the few examples that deal with the effects of inspection capability and inspection scheduling on probabilistic damage tolerant design. To date, however, little research has been published investigating the interaction of inspection probability and actual and

detected damage size distributions for composite structures. Furthermore, statistical methods are available that would enable the use of service inspection data to update the structural safety risk for a fleet of aircraft on a continuous basis. The work presented here proposes a simplified approach for defining damage tolerant structural safety based on a probabilistic characterization of damage sizes and detection methods. Bayesian statistics are applied to the probability distributions to update the design reliability results as new damage size data become available.

Formulation

Modern damage-tolerant design philosophy requires that damage accumulated during the service life of a component be detected and repaired before the strength of the component is degraded beyond some design threshold. A good way to quantify the relative safety of a structure is with the term level of safety (LS), which is defined as the compliment of the probability that a flaw size larger than the critical flaw size for residual strength of the structure is incurred and that the flaw will not be detected[5]:

$$\mathrm{LS} = 1 - \mathrm{PF} = 1 - P(A \geq a_c, D = 0) \tag{1}$$

In this context, LS refers strictly to the reliability of detecting all damage sizes greater than critical. This definition assumes that only a single flaw is present and that it is not growing with time. The probability of failure (PF) is the joint probability of detection state and damage size:

$$\mathrm{PF} = P(A \geq a_c, D = 0) = \int_{a_c}^{\infty} f_{D,A}(0, a)\, \mathrm{d}a \tag{2}$$

The detection state is a binary random variable and is conditional on the size of the damage present,

$$f_{D,A}(0, a) = f_D(0 \mid a) f_A(a) \tag{3}$$

Redefining the probability density functions (PDFs) and substituting gives the definition for PF

$$P_D(a) = f_D(1 \mid a) \tag{4}$$

$$p(a) = f_A(a) \tag{5}$$

$$\mathrm{PF} = \int_{a_c}^{\infty} p(a)[1 - P_D(a)]\, \mathrm{d}a \tag{6}$$

This form of the relation between damage detection capability and damage size distribution was investigated by Berens and Hovey for cracks in metal aircraft structures.[6] However, the derivation is such that it is general enough to be applicable to any structural damage mechanism that can be parameterized by a single characteristic dimension.

The distribution of actual damage in a structure can never be completely characterized because the observed damage sizes are always filtered through the detection probability of the particular nondestructive evaluation (NDE) technique being used. An alternative formulation for the PF can be derived that is independent of actual damage size distribution. The joint distribution of detection state and damage size can be rewritten using Bayes's law as

$$f_D(1 \mid a) f_A(a) = f_A(a \mid 1) f_D(1) \tag{7}$$

Redefining the PDFs and rearranging gives a definition for the actual damage size distribution:

$$p_0(a) = f_A(a \mid 1) \tag{8}$$

$$p(a) = f_D(1)[p_0(a)/P_D(a)] \tag{9}$$

For Eq. (9) to be a valid PDF, both sides of the equation must integrate to one. This yields a value for a normalizing constant that is defined as

$$f_D(1) = \left\{ \int_0^{\infty} \frac{p_0(a)}{P_D(a)}\, \mathrm{d}a \right\}^{-1} \tag{10}$$

Substituting for the actual damage size distribution, the new PF relation is

$$\mathrm{PF} = \int_{a_c}^{\infty} \frac{p_0(a)}{P_D(a)}[1 - P_D(a)]\, \mathrm{d}a \Big/ \int_0^{\infty} \frac{p_0(a)}{P_D(a)}\, \mathrm{d}a \tag{11}$$

The definition for LS presented so far assumes a single inspection event at a fixed point in time and that only a single discrete-source flaw is present in the structure. If the LS for a single flaw in a structural detail is given by the value p, then the probability of finding z flaws in a structure that has n flaws present is given by a binomial distribution, assuming each flaw is independent of the others:

$$P(Z = z) = \binom{n}{z} p^z (1 - p)^{n - z} \tag{12}$$

For structural safety, all of the flaws larger than the critical size must be detected, so that $z = n$ and

$$P(Z = n) = p^n \tag{13}$$

By analogy, the overall LS for multiple flaws can then be rewritten as

$$\mathrm{LS} = \{1 - \mathrm{PF}\}^{\mu} \tag{14}$$

For multiple damage mechanisms and damage locations in a structure, the overall LS is the product of all of the individual LS values:

$$\mathrm{LS} = \prod_{i=1}^{N_L} \prod_{j=1}^{N_{T_i}} \{1 - \mathrm{PF}_{ij}\}^{\mu_{ij}} \tag{15}$$

Probability Models

The equations that so far define the concept of LS [Eqs. (1), (6), (11), and (15)] are general enough to be applicable to any damage type or structural configuration, when it is assumed that the residual strength behavior and damage detection characteristics can be parameterized by a single characteristic dimension. The choice of which probability models to use in the formulas, however, is dependent on the damage mechanism being modeled, structural configuration, material system, operating condition, loading, and any other constraints relevant to the damage-tolerance problem. Berens and Hovey[7] and Berens[8] have conducted extensive research to characterize probability of detection (POD) models for cracks in metal aircraft structures, with a cumulative lognormal distribution used to model hit/miss response data. Rummel and Matzkanin approximate the lognormal distribution by a log-odds model.[9] Unfortunately, efforts to extend this work to composites have so far been minimal. For the purposes of this analysis, the lognormal/log-odds model is assumed to apply equally well to composites in this study.

The form of the POD model is such that the POD goes to zero as the damage size approaches either zero or some minimum detection threshold. The PDF of detected damage $p_0(a)$ will also go to zero then, as the damage size approaches zero. When Eq. (9) is examined, it can be seen that the form of the PDF for actual damage $p(a)$ is proportional to the rates at which the POD curve and the detected damage PDF approach zero. If the POD curve goes to zero faster than the detected damage PDF, then the PDF for actual damage will asymptotically go to infinity as the damage size approaches zero. This may in fact be the correct behavior for the actual damage size distribution, but the order of singularity must be such that the normalizing constant [Eq. (10)] is integrable over the entire domain of damage sizes. This requirement could prove difficult to enforce under experimental conditions. In such cases, the PF formulation of Eq. (6) should be used, where a PDF for actual damage can be assumed that will be integrable under all cases. As a result, Eqs. (1) and (6) should be considered the general case LS formulation and Eqs. (1) and (11) a special case where the actual damage size distribution is known to go to zero as the damage size approaches zero. For this analysis, the special case is assumed because of its simplified Bayesian mathematics and the better observability of the data distributions.

Composite Damage

To demonstrate the LS approach to structural design, a composite material system was chosen for investigation. It is felt that the highest potential payoff of the LS approach may be realized in its application to composite design, because of the large knock-down factors typically used and the higher degree of uncertainty relative to metal designs. A generic graphite–epoxy honeycomb sandwich was selected for study because this is the dominant type of high-performance composite structure on commercial aircraft, and so service-induced damage data derived from the commercial fleet will be most applicable to this configuration. Very little quantitative data exist on the distribution of damage sizes in various composite structural applications. One of the few published examples of such data is found in Ref. 1. Damage size data were presented for holes, cracks, and delaminations in composite aircraft structures, based on a qualitative survey of maintenance technicians at various airline and U.S. Navy repair facilities. An excerpt of this data is reprinted in Table 1, in modified form.

Two-parameter probability models for detected damage size may be fitted to the composite damage types based on the data in Table 1. Because of the nature of the data, the type of probability models that best fit the distribution of damage sizes cannot be determined, and must be assumed. Lognormal or Weibull PDFs are often used to model damage size distributions, and so a lognormal model will be used here for detected damage size distribution, with a model form of

$$p_0(a) = \frac{1}{a\sigma\sqrt{2\pi}}\exp\left[-\frac{1}{2\sigma^2}\ln^2\left(\frac{a}{\theta}\right)\right] \tag{16}$$

The values of the model parameters derived from the data in Table 1 are shown in Table 2. The resulting damage size distributions are plotted in Fig. 1.

The log-odds distribution is the detection probability model used for the composite damage types. The original form is given by

$$P_D(a) = \frac{\exp[\alpha + \beta \ln(a)]}{1 + \exp[\alpha + \beta \ln(a)]} \tag{17}$$

The constants α and β can be reparameterized to yield the form

$$P_D(a) = \frac{(a/a_{50})^k}{1 + (a/a_{50})^k} \tag{18}$$

The values of the parameters used in the log-odds model for each damage type are assumed based on the shape of the detected damage distributions derived from Table 1 data. The detected damage distributions are dependent on the type of inspection method used to collect the data; however, Ref. 1 does not specify methods of detection for the published figures. The curves used here are assumed to represent visual inspection methods for hole and crack damage and some combination of visual and tap testing for delamination damage. The parameter values in the log-odds model are chosen to represent detection probabilities that can be reasonably obtained for operational inspections and that would likely result in the shapes of the damage size distributions observed. Parameter values are listed in Table 3. The POD distributions are plotted in Fig. 2.

When the form of the log-odds model in Eq. (18) is used combined with the lognormal detected damage model [Eq. (17)], a formula for the actual damage distribution may be found by solving Eq. (9):

$$q = (a_{50}/\theta)^k \exp(k^2\sigma^2/2)$$

$$p(a) = \log N(a;\theta,\sigma) + q\log N[a;\theta\exp(-k\sigma^2),\sigma]/(1+q) \tag{19}$$

Generally, closed-form solutions for $p(a)$ cannot be obtained, and Eq. (9) must be solved numerically. The actual damage distributions are plotted in Fig. 3.

With the probability distributions for the composite damage types defined, the LS for each damage type can be calculated as a function of critical damage size. Using Eqs. (1) and (11), the LS was integrated numerically with the SLATEC DQAGI subroutine in FORTRAN. Absolute and relative accuracy for each integration calculation was 10^{-12}. The resulting values are plotted as a function of critical damage size in Fig. 4.

Table 1 Composite damage size data from Ref. 1

	Damage size, in.		
Damage type	<1.5	1.5–3.0	>3.0
Hole damage, %	51.4	34.3	14.3
Delaminations, %	11.1	31.1	57.8
Cracks, %	30	30	40

Table 2 Parameters for lognormal detected damage size distributions

Damage type	θ	σ
Hole damage	1.465	0.672
Delaminations	3.427	0.677
Cracks	2.394	0.891

Table 3 Parameters for log-odds detection probability distributions

Damage type	a_{50}	k
Hole damage	0.5	2.5
Delaminations	2.0	2.6
Cracks	0.8	1.8

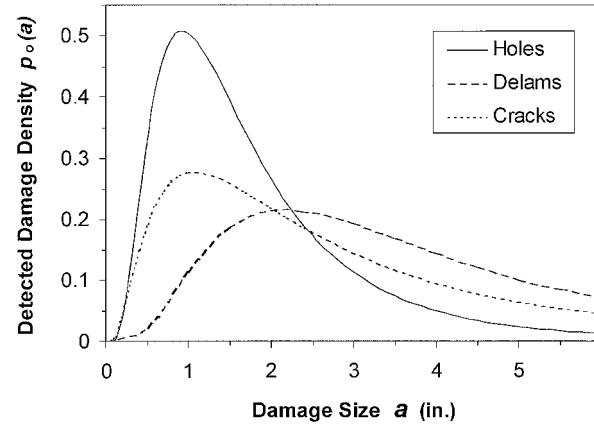

Fig. 1 Lognormal PDF for baseline fleet damage.

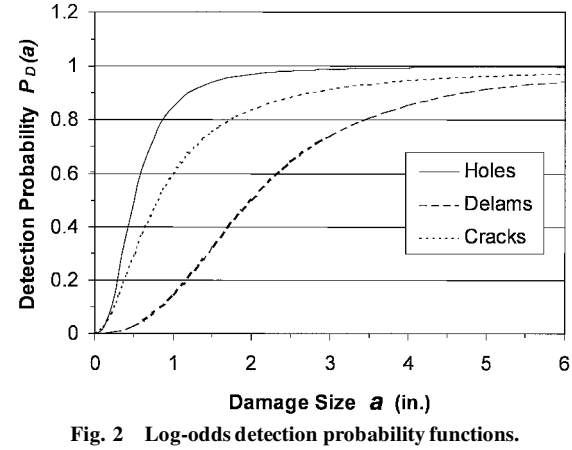

Fig. 2 Log-odds detection probability functions.

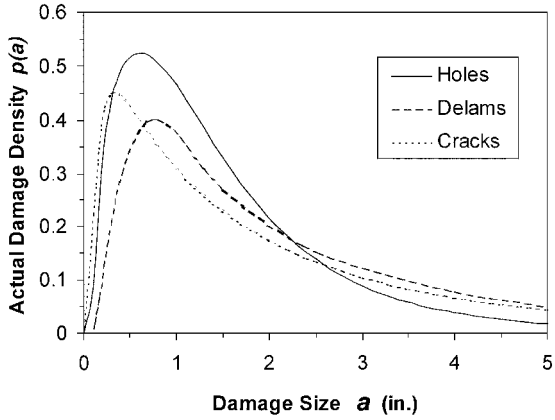

Fig. 3 PDF for actual damage size.

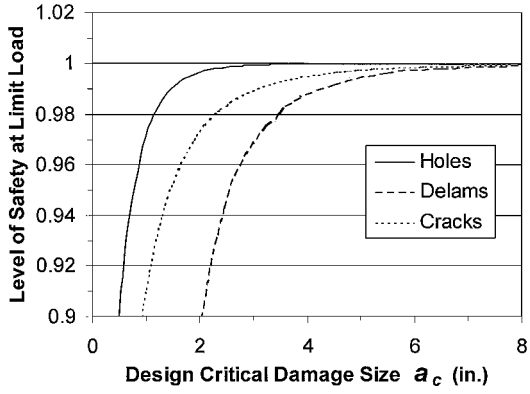

Fig. 4 LS vs critical damage size for composite damage types.

Residual Strengths

When structures are designed using the LS approach, an appropriate critical damage size for each damage type must be chosen based on the service loads and the structural LS desired. Deterministic analyses of residual strengths as a function of damage size must be performed to provide the data necessary for making design trades to meet the safety requirements of the structure. For this demonstration, a graphite–epoxy laminate with a Nomex honeycomb core will be analyzed. Individual ply properties are as follows.

Tension:

$$E_1 = 22.9 \text{ Mpsi}, \qquad E_2 = 1.34 \text{ Mpsi}, \qquad \nu_{12} = 0.34$$

$$G_{12} = 0.29 \text{ Mpsi}, \qquad X = 350 \text{ ksi}$$

$$\varepsilon_L = 15{,}300\mu\varepsilon, \qquad \varepsilon_T = 5{,}680\mu\varepsilon, \qquad \gamma_{LT} = 21{,}000\mu\varepsilon$$

Compression:

$$E_1 = 22.0 \text{ Mpsi}, \qquad E_2 = 1.34 \text{ Mpsi}, \qquad \nu_{12} = 0.34$$

$$G_{12} = 0.29 \text{ Mpsi}, \qquad X' = 295 \text{ ksi}$$

$$\varepsilon'_L = 13{,}500\mu\varepsilon, \qquad \varepsilon'_T = 5{,}680\mu\varepsilon, \qquad \gamma'_{LT} = 21{,}000\mu\varepsilon$$

Individual ply thickness is 0.005 in. Laminate thickness is chosen as the structural sizing parameter of interest, and three different stacking sequences are specified to provide a range of thicknesses for design trades: laminate 1 $[-45/0/45/0/90]_s$, laminate 2 $[-45/0/45/90]_{2s}$, and laminate 3 $[-45/0/45/0/90]_{2s}$.

Core stiffness was varied for each laminate to prevent global buckling of damaged specimens during analysis. Core thickness was 1.0 in. for all laminates. Core properties are as follows.

Core 1:

$$E_1 = E_2 = 200 \text{ psi}, \qquad E_3 = 20 \text{ ksi}$$

$$\nu_{12} = 0.5, \qquad \nu_{13} = \nu_{23} = 0.01$$

$$G_{12} = 20 \text{ psi}, \qquad G_{13} = 7 \text{ ksi}, \qquad G_{23} = 3.5 \text{ ksi}$$

Core 2:

$$E_1 = E_2 = 600 \text{ psi}, \qquad E_3 = 60 \text{ ksi}$$

$$\nu_{12} = 0.5, \qquad \nu_{13} = \nu_{23} = 0.01$$

$$G_{12} = 60 \text{ psi}, \qquad G_{13} = 13 \text{ ksi}, \qquad G_{23} = 6 \text{ ksi}$$

Core 3:

$$E_1 = E_2 = 900 \text{ psi}, \qquad E_3 = 90 \text{ ksi}$$

$$\nu_{12} = 0.5, \qquad \nu_{13} = \nu_{23} = 0.01$$

$$G_{12} = 90 \text{ psi}, \qquad G_{13} = 17 \text{ ksi}, \qquad G_{23} = 9 \text{ ksi}$$

Undamaged tensile and compressive strengths of the laminates were calculated using first-ply failure theory. Three types of damage were analyzed for the given laminates: core/facesheet disbonding, facesheet delamination, and notches. Disbonding was assumed only for a single facesheet, and delaminations were assumed only at the mid-plane of a single facesheet. Notch damage was analyzed for both a single facesheet and for notches through both facesheets and the core. For each damage type, circular and elliptical damage areas were modeled. Elliptical damage areas have a constant 3:1 ratio of major to minor axes dimensions, with the major axis oriented perpendicular to the loading direction. An 18×24 in. flat panel specimen was used for the analysis, with all damages centered on the panel and loading applied in the lengthwise direction.

To facilitate the investigation of a large number of data points, a simplified engineering approach was used in calculating residual strengths for the various damage types. Postbuckling residual strengths for delamination and disbond cases are determined assuming that the buckled area carries a constant load until global failure is reached. The strain concentration at the buckled edges is calculated using finite element models of the panel, with failure determined when the notch-tip strain exceeds the allowable value. Strength values for the notched cases were determined using the Mar–Lin fracture model, with the model parameters modified using geometric corrections derived from finite element models of the damaged panels. Details of the analysis approach and validation may be found in Ref. 5.

Results of the deterministic residual strength analyses are shown in Figs. 5–8, with the data points for elliptical damage plotted as a function of equivalent circular diameter (dashed lines). Residual strength results for notches through the total panel thickness are not plotted because these values are similar to those for notches through a single facesheet.

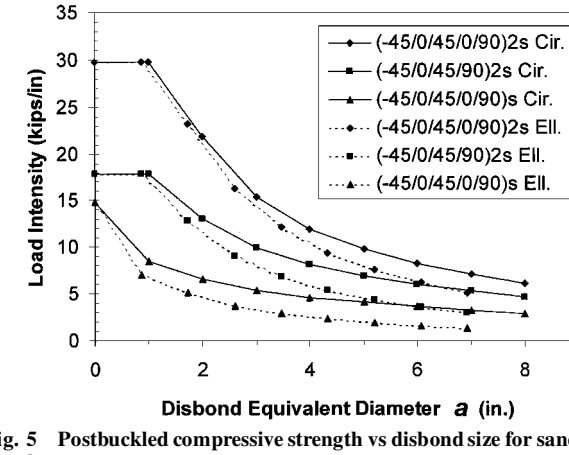

Fig. 5 Postbuckled compressive strength vs disbond size for sandwich panel.

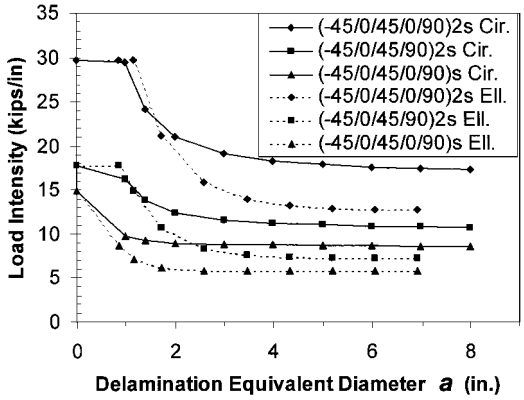

Fig. 6 Postbuckled compressive strength vs delamination size for sandwich panel.

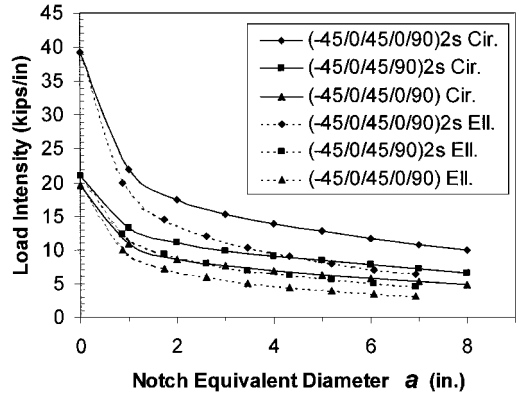

Fig. 7 Tensile residual strength of sandwich panel with notch on one facesheet.

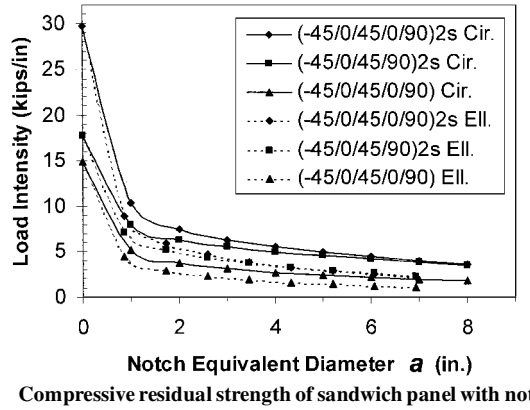

Fig. 8 Compressive residual strength of sandwich panel with notch on one facesheet.

Failure Probabilities

With the residual strengths of the various damage types plotted as a function of damage size, and the LS for each damage type calculated as a function of critical damage size, a critical damage size for each damage type must be chosen to yield an appropriate safety value at the operating load of the structure. Design charts of LS as a function of limit load can be constructed by cross plotting the residual strength values as a function of LS. These plots are shown in Figs. 9–12 for each damage type investigated. Failure probabilities are the independent variables used in the charts, because the plot results are much easier to interpret than using LS values. The shapes of the plots are a function of the residual strength behavior and the damage size distributions used in the probabilistic calculations. Delamination probability calculations are also applied to disbond damage.

The results indicate that a substantial reduction in residual strength compared to undamaged sandwich strength must be accepted before high LS can be realized. This is largely due to the nature of the data used to estimate the damage size distributions.

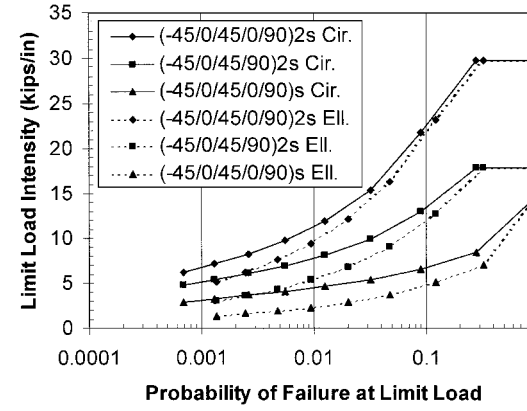

Fig. 9 Compressive failure probability for disbonded sandwich panel.

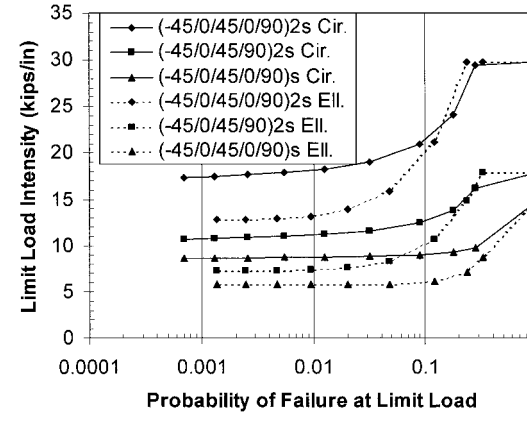

Fig. 10 Compressive failure probability for delaminated sandwich panel.

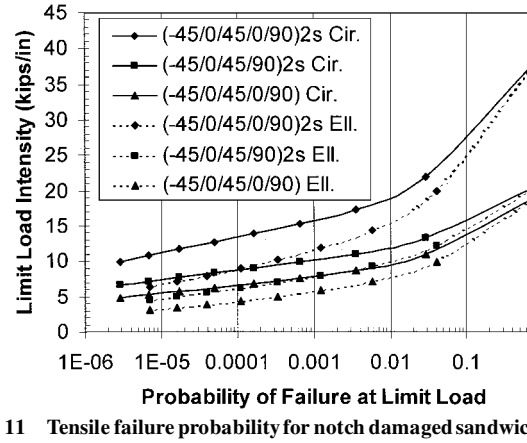

Fig. 11 Tensile failure probability for notch damaged sandwich panel.

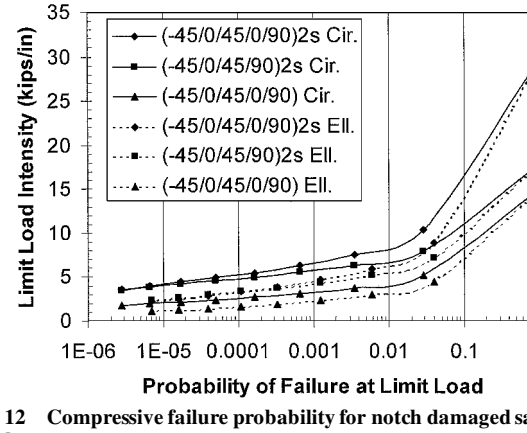

Fig. 12 Compressive failure probability for notch damaged sandwich panel.

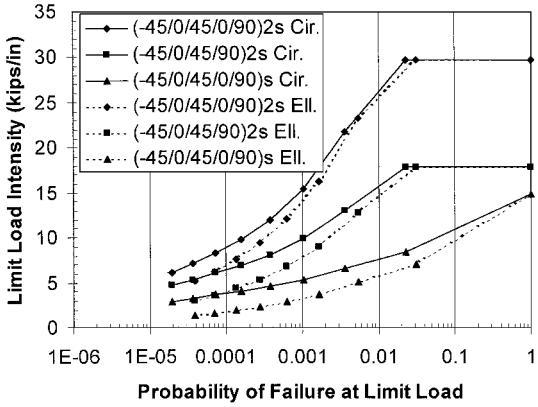

Fig. 13 Compressive failure probability for disbonded panel (NDE inspection).

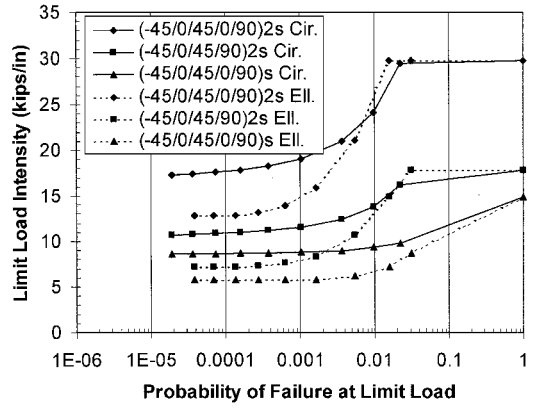

Fig. 14 Compressive failure probability for delaminated panel (NDE inspection).

Damage size data from Ref. 1 represent an aggregate of all carbon–fiber and glass-fiber reinforced composite structures in service with the commercial aircraft fleet. As a result, well-designed structures with high levels of damage resistance are excessively penalized by poorer performing structures or structures that are located in areas with high damage accumulation rates. In practice, zoning procedures are generally used to relate damage characteristics to particular locations on an aircraft and would reduce much of the conservatism shown in the plotted results.

Lower failure probabilities for disbond and delamination damage can be found by assuming a POD curve representing an automated NDE method for detecting these types of damages. Using the log-odds model, parameters chosen for the NDE POD are

$$a_{50} = 0.5, \qquad k = 2.6$$

Failure probabilities are calculated using the NDE detection model and the actual damage distribution estimated from the visual/tap-test POD model. Results are shown in Figs. 13 and 14.

Example Problem

The design charts shown in Figs. 9–14 are useful in sizing a composite sandwich structure for given loading and safety requirements. For example, suppose a compression panel is being designed to withstand an average limit load of 3000 lb/in. (location I) and a load concentration of 10,000-lb/in. limit at a particular location (location II). The panel is subject to disbond and delamination type damage at both locations, and visual/tap-test inspections are the preferred method of detecting the damage. The allowable LS for the entire panel is 99.8% at limit load. When Figs. 9 and 10 are the starting point, it can be seen that disbonding is the more critical damage type compared to delamination. From Fig. 9, the thinnest sandwich facesheet that will support the average 3000-lb/in. limit load and still exceed minimum safety criteria is the $(-45/0/45/90)_{2S}$ layup. This choice of facesheet will yield a maximum PF at limit load of $\mathrm{PF}_I = 0.0015$, for a single disbond at location I. Equation (15) can be used to calculate the remaining safety margin available to size the structure at the load concentration:

$$\mathrm{LS} = (1 - \mathrm{PF}_I)^1 (1 - \mathrm{PF}_{II})^1$$

$$0.998 = (1 - 0.0015)^1 (1 - \mathrm{PF}_{\text{II-allow}})^1$$

To maintain overall structural safety, the allowable PF at location II is now $\mathrm{PF}_{\text{II-allow}} = 5.01 \times 10^{-4}$. From Fig. 9, it is clear that the required failure probability for location II cannot be obtained using strictly visual/tap-test inspection methods. Instead, an automated NDE technique can be specified at location II, which would improve the failure probability results enough to meet design safety requirements (Fig. 13). Changing the sandwich facesheet to a $(-45/0/45/0/90)_{2S}$ layup at location II, the maximum PF at the 10,000-lb/in. limit load is $\mathrm{PF}_{II} = 3.1 \times 10^{-4}$ for a single disbond at location II (from Fig. 13). The overall LS for the structure can now be calculated using Eq. (15):

$$\mathrm{LS} = (1 - \mathrm{PF}_I)^1 (1 - \mathrm{PF}_{II})^1$$

$$= (1 - 0.0015)(1 - 3.1 \times 10^{-4}) = 0.9982$$

Because the calculated LS value is greater than the allowable value, the new structure meets the design criteria for safety. This simple example illustrates the interaction between damage size distributions, inspection methods, structural sizing parameters, that is, facesheet thickness, and overall safety that is encompassed in a damage tolerance problem. The example also demonstrates how an equivalent LS approach can be used to optimize structural performance for a given set of design and safety constraints.

Bayesian Updating

During the preliminary design phase, little information may be available on the damage tolerance behavior of the evolving design. LS calculations during this phase will have a high degree of uncertainty associated with the predictions of damage sizes experienced in service. Bayesian updating provides a powerful statistical tool for revising probability distributions and reducing uncertainty when new data become available for use. In Bayesian updating, the parameters that define the distribution shape in a particular probability model are themselves treated as random variables, with their own probability distributions. New damage size data points are used to reduce the variance of the parameter distributions, with the result that the damage size distribution is revised to represent a weighted average of the old and new data. This technique has been previously demonstrated by Cruse for initial crack depths on a center-cracked panel problem.[10]

For the detected damage size distribution with a_n new damage size data points, the updated joint PDF of the model parameters are

$$f_u(\theta, \sigma \mid a_1, a_2, \ldots, a_n) \propto \prod_{i=1}^{n} p_0(a_i \mid \theta, \sigma) f_0(\theta, \sigma) \qquad (20)$$

The updated probability distributions for each model parameter can be found by integrating out the unwanted parameters from the updated joint PDF. The Bayesian updated values for the model parameters are simply the means of each marginal parameter distribution. For the lognormal detected damage size model chosen before, the log of the damage size is distributed normally:

$$y = \log(a) \sim N(\mu, \sigma^2) \qquad (21)$$

$$\mu = \log(\theta) \qquad (22)$$

Conjugate prior distributions along with the joint and marginal posterior distributions for the normal probability model have been derived by Gelman et al.[11] The lognormal variance parameter σ^2 is distributed scaled inverse χ^2, and the lognormal mean parameter μ is distributed normally, but is conditional on the prior value of the variance parameter:

$$\mu \mid \sigma^2 \sim N(\mu_0, \sigma^2/\kappa_0) \qquad (23)$$

$$\sigma^2 \sim \text{inv}\,\chi^2\left(\nu_0, \sigma_0^2\right) \qquad (24)$$

When these distributions are applied to Eq. (20), the updated joint PDF of the model parameters is distributed,

$$\mu, \sigma^2 \mid y \sim N \cdot \text{inv}\chi^2\left(\mu_n, \sigma_n^2/\kappa_n; \nu_n, \sigma_n^2\right)$$

$$\mu_n = [\kappa_0/(\kappa_0 + n)]\,\mu_0 + [n/(\kappa_0 + n)]\bar{y}$$

$$\kappa_n = \kappa_0 + n, \qquad \nu_n = \nu_0 + n$$

$$\nu_n\sigma_n^2 = \nu_0\sigma_0^2 + (n-1)s^2 + [\kappa_0 n/(\kappa_0 + n)](\bar{y} - \mu_0)^2 \quad (25)$$

where the new data points are represented in the equations by the sample mean and variance, respectively,

$$\bar{y} = \frac{1}{n}\sum_{i=1}^{n}\log(a_i) \quad (26)$$

$$s^2 = \frac{1}{n-1}\sum_{i=1}^{n}[\log(a_i) - \bar{y}]^2 \quad (27)$$

Note that the updated joint PDF parameters are weighted averages of the old and new damage data. The posterior marginal distributions of the lognormal model parameters are

$$\mu \mid y \sim t_{\nu_n}\left(\mu_n, \sigma_n^2/\kappa_n\right) \quad (28)$$

$$\sigma^2 \mid y \sim \text{inv}\chi^2\left(\nu_n, \sigma_n^2\right) \quad (29)$$

where μ is Student-t distributed. To demonstrate this method, delamination damage data are assumed to be collected for a particular structure of interest. The damage sizes are 1.5, 2.2, 2.7, 3.2, and 5.4 in. The sample mean and variance are calculated using Eqs. (26) and (27), with the resulting values of

$$\bar{y} = 1.007 \qquad s^2 = 0.2239$$

The prior detected damage size distribution is defined by the lognormal delamination model parameters from Table 2. Three levels of uncertainty in the prior damage size distribution are assumed (levels I–III) and are shown in Table 4 in order of increasing uncertainty. The level of uncertainty is quantified by specifying either the variance or the standard deviation of the lognormal model parameter distributions [Eqs. (23) and (24)]. In this example, the quantities are expressed as some percentage of the mean. The resulting parameter values for the distributions in Eqs. (23) and (24) are calculated and shown in Table 4.

The lognormal model parameter distributions are plotted in Figs. 15 and 16 and show that, as the level of uncertainty increases, the distributions become flatter and more dispersed. The new damage size data is then used to update the parameter distributions using Eq. (25), with the results shown in Table 4. The new, updated values of the lognormal damage size model parameters θ and σ^2 are the means of the marginal posterior distributions in Eqs. (28) and (29). These values are also shown in Table 4. The prior detected

Table 4 Inputs and results of Bayesian updating of detected delamination size distribution for varying levels of uncertainty

Parameters	Level I	Level II	Level III
Prior standard deviation of θ	15% mean	30% mean	45% mean
Prior variance of σ^2	10% mean	25% mean	100% mean
μ_0	1.221	1.189	1.139
κ_0	20.60	5.318	2.485
ν_0	13.17	7.667	4.917
σ_0^2	0.3887	0.3388	0.2719
μ_n	1.179	1.101	1.051
κ_n	25.60	10.32	7.485
ν_n	18.17	12.67	9.917
σ_n^2	0.3411	0.2824	0.2281
Updated θ	3.251	3.006	2.861
Updated σ^2	0.3833	0.3354	0.2857

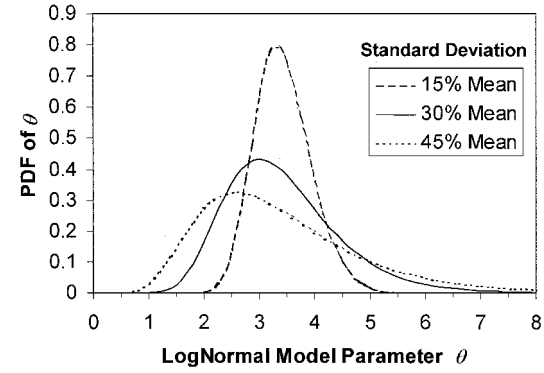

Fig. 15 Conditional Distribution of median delamination parameter θ for changes in standard deviation.

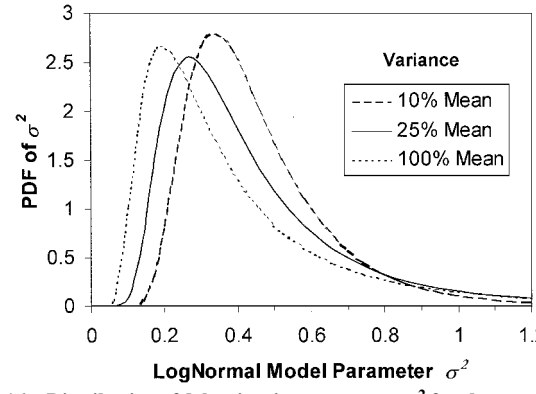

Fig. 16 Distribution of delamination parameter σ^2 for changes in variance.

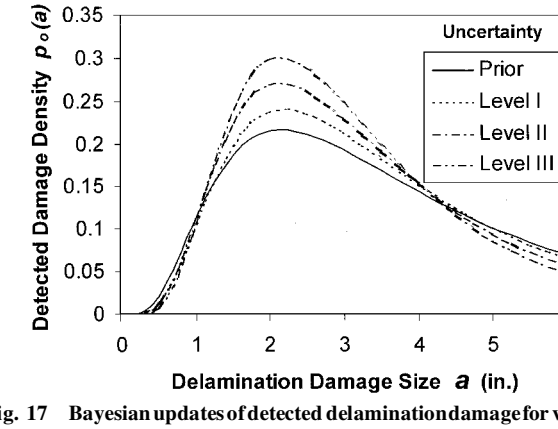

Fig. 17 Bayesian updates of detected delamination damage for varying levels of uncertainty.

delamination size distribution is plotted along with the updated distributions for the various uncertainty levels in Fig. 17. The results show that, as the level of uncertainty in the prior distribution increases, the updated distribution is weighted more heavily toward the new data. The updated damage size distribution can then be used to recalculate the LS values for the structure with the new damage size data points incorporated. Note that Bayesian analysis cannot determine the appropriate probability model to use for the damage size distribution. This can only be accomplished through detailed data collection and analysis of the damage behavior.

Design Procedure

Based on the analysis of the composite sandwich structure shown here, a process for damage tolerant design using the equivalent LS methodology has been proposed and is shown in the flowchart of Fig. 18. For the design of a new structure, distributions of damage sizes, number of occurrences, and detection probabilities are initially

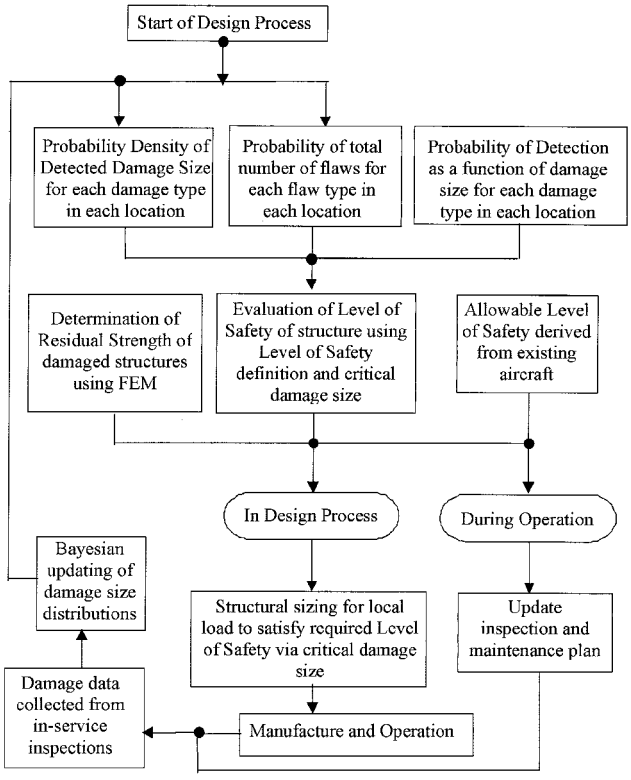

Fig. 18 Flowchart for damage tolerant design using equivalent LS methodology.

assumed based on available data. Deterministic analyses using finite element methods and/or structural tests are performed to characterize residual strength as a function of the relevant structural sizing parameters. If the new structure is intended to replace an older structure, an allowable value for the LS of the new structure can be obtained by performing a separate LS analysis on the existing structure. The LS of the new structure must then meet or exceed the allowable value. If the LS for an existing structure is not obtainable, then an allowable value should be chosen based on the level of structural safety risk the designer is willing to accept. The deterministic residual strength results are then combined with the probabilistic damage and inspection data to size the structure for the required load and safety level. Once the structure has been built and put into service, damage data can be collected from the periodic maintenance inspections necessary for damage-tolerant structures. This service inspection data can be used with Bayesian updating to recalculate the LS value for the structure, resulting in a quantitative measure of safety that is based on the structure's actual performance in service. Although the structure cannot be resized to take advantage of the new damage data, inspection and maintenance procedures can be optimized to maintain an equivalent LS throughout the life of the structure.

Conclusions

The equivalent LS design methodology discussed here is an extension of reliability theory and statistical analysis tools to the design and maintenance of damage-tolerant aircraft structures. The method presents a unified approach to damage tolerance that allows a direct comparison of relative safety between structures using different materials, construction techniques, loading, or operational conditions. Service inspection capabilities are incorporated directly into the design process. The use of Bayesian statistical tools provides a mechanism for validating the damage size assumptions made during the design process and for reducing the level of uncertainty and risk over the lifecycle of the structure. The analysis results demonstrate the applicability of the method in characterizing damage uncertainty in composite structural design and show how a quantitative measure of safety can be utilized in the design process to optimize structural performance. The results also demonstrate that more effort must be made to collect detailed service damage data for composite damage mechanisms and to investigate the probability models that best fit the data. More work must also be done to extend the method to include damage growth rates, variable rates of damage accumulation, inspection scheduling, and other variables. However, the underlying methodology has broad potential application to damage-tolerant aircraft structural design with uncertainty.

Acknowledgments

This work was supported by the NASA Langley Research Center under Grant NAG-1-2055. The authors wish to thank W. J. Stroud of NASA, Bjorn Backman of The Boeing Company (retired), Larry Ilcewicz and David Swartz of the Federal Aviation Administration and Greg Ridgeway of the University of Washington for their invaluable support in this research effort.

References

[1]Gray, P. M., and Riskalla, M. G., "Development of Probabilistic Design Methodology for Composite Structures," Federal Aviation Administration, DOT/FAA/AR-95/17, Washington, DC, Aug. 1997.

[2]Long, M. W., and Narciso, J. D., "Probabilistic Design Methodology for Composite Aircraft Structures," Federal Aviation Administration, DOT/FAA/AR-99/2, Washington, DC, June 1999.

[3]Rouchon, J., "Certification of Large Airplane Composite Structures, Recent Progress and New Trends in Compliance Philosophy," *Proceeding of the 17th ICAS Congress*, Vol. 2, AIAA, Washington, DC, 1990, pp. 1439–1447.

[4]Ushakov, A., Kuznetsov, A., Stewart, A., and Mishulin, I., "Probabilistic Design of Damage Tolerant Composite Aircraft Structures (ProDeCompoS); Final Report under Annex 1 to Memorandum of Cooperation AIA/CA-71 between the Federal Aviation Administration (FAA) and the Central Aerohydrodynamic Institute (TsAGI)," Central Aerohydrodynamic Inst., Moscow, 1996.

[5]Lin, K. Y., Du, J., and Rusk, D. T., "Structural Design Methodology Based on Concepts of Uncertainty," NASA CR-2000-209847, Langley, VA, Feb. 2000.

[6]Berens, A. P., and Hovey, P. W., "Quantifying NDI Capability for Damage Tolerance Analysis," *Review of Progress in Quantitative Nondestructive Evaluation*, Vol. 3A, Plenum, New York, 1984, pp. 25–35.

[7]Berens, A. P., and Hovey, P. W., "Statistical Methods for Estimating Crack Detection Probabilities," *Probabilistic Fracture Mechanics and Fatigue Methods: Applications for Structural Design and Maintenance*, ASTM, STP 798, American Society for Testing and Materials, Philadelphia, 1983, pp. 79–94.

[8]Berens, A. P., "NDE Reliability Data Analysis," *Nondestructive Evaluation and Quality Control*, edited by S. R. Lampman and T. B. Zorc, Vol. 17, Metals Handbook, 9th ed., ASM International, Metals Park, OH, 1989, pp. 689–701.

[9]Rummel, W. D., and Matzkanin, G. A., *Nondestructive Evaluation (NDE) Capabilities Data Book*, 3rd ed., Nondestructive Testing Information Analysis Center, Austin, TX, 1997, pp. 6–2, 6-3.

[10]Harris, D. O., "Probabilistic Crack Growth and Modeling," *Reliability-Based Mechanical Design*, edited by T. A. Cruse, Marcel Dekker, New York, 1997, pp. 300–311.

[11]Gelman, A., Carlin, J. B., Stern, H. S., and Rubin, D. B., *Bayesian Data Analysis*, Chapman and Hall, New York, 1995, pp. 71–73.